Atmos. Meas. Tech. Discuss., 3, 5613–5643, 2010
www.atmos-meas-tech-discuss.net/3/5613/2010/
doi:10.5194/amtd-3-5613-2010

Atmospheric Measurement Techniques Discussions

Preliminary validation of column-averaged volume mixing ratios of carbon dioxide and methane retrieved from GOSAT short-wavelength infrared spectra

I. Morino[1], O. Uchino[1], M. Inoue[1], Y. Yoshida[1], T. Yokota[1], P. O. Wennberg[2], G. C. Toon[3], D. Wunch[2], C. M. Roehl[2], J. Notholt[4], T. Warneke[4], J. Messerschmidt[4], D. W. T. Griffith[5], N. M. Deutscher[5], V. Sherlock[6], B. Connor[6], J. Robinson[6], R. Sussmann[7], and M. Rettinger[7]

[1]National Institute for Environmental Studies, 16-2 Onogawa, Tsukuba, Ibaraki, 305-8506, Japan
[2]California Institute of Technology, Pasadena, California, 91125-2100, USA
[3]Jet Propulsion Laboratory, California Institute of Technology, 4800 Oak Grove Drive, Pasadena, California, 91109-8099, USA

[4]Institute of Environmental Physics, University of Bremen, 28334 Bremen, Germany
[5]Center for Atmospheric Chemistry, University of Wollongong,
New South Wales, 2522, Australia
[6]National Institute of Water and Atmospheric Research, Wellington, New Zealand
[7]IMK-IFU, Karlsruhe Institute of Technology, Garmisch-Partenkirchen, Germany

Received: 26 November 2010 – Accepted: 30 November 2010 – Published: 8 December 2010

Correspondence to: O. Uchino (uchino.osamu@nies.go.jp)

Published by Copernicus Publications on behalf of the European Geosciences Union.

Abstract

Column-averaged volume mixing ratios of carbon dioxide and methane retrieved from the Greenhouse gases Observing SATellite (GOSAT) Short-Wavelength InfraRed observation (GOSAT SWIR X_{CO2} and X_{CH4}) were compared with the reference data obtained by ground-based high-resolution Fourier Transform Spectrometers (g-b FTSs) participating in the Total Carbon Column Observing Network (TCCON).

Through calibrations of g-b FTSs with airborne in-situ measurements, the uncertainty of X_{CO2} and X_{CH4} associated with the g-b FTS was determined to be 0.8 ppm (~0.2%) and 4 ppb (~0.2%), respectively. The GOSAT products are validated with these calibrated g-b FTS data. Preliminary results are as follows: The GOSAT SWIR X_{CO2} and X_{CH4} (Version 01.xx) are biased low by 8.85 ± 4.75 ppm (2.3 ± 1.2%) and 20.4 ± 18.9 ppb (1.2 ± 1.1%), respectively. The precision of the GOSAT SWIR X_{CO2} and X_{CH4} is considered to be about 1%. The latitudinal distributions of zonal means of the GOSAT SWIR X_{CO2} and X_{CH4} show similar features to those of the g-b FTS data.

1 Introduction

The concentration of carbon dioxide (CO_2) has increased from about 280 to 380 ppm over the past century due to the burning of fossil fuels associated with expanding industrial activities (IPCC, 2007). CO_2 absorbs the infrared radiation from the surface and hence an increase in the CO_2 concentration leads to a rise in atmospheric temperature. CO_2 and other trace gases such as methane (CH_4), nitrous oxide (N_2O), hydrofluorocarbons (HFCs), perfluorocarbons (PFCs) and sulfur hexafluoride (SF_6) are greenhouse gases that are subject to emission regulations under the Kyoto Protocol. Together, CO_2 and CH_4 account for over 80 percent of the total warming effect caused by all greenhouse gases based on the estimates of radiative forcing from 1750 to 2005 (IPCC, 2007). Changes in temperature can cause feedbacks that alter CO_2 concentrations by influencing the biosphere (Cox et al., 2000). To accurately predict future

AMTD
3, 5613–5643, 2010

atmospheric CO_2 concentrations and their impacts on climate, it is necessary to clarify the distribution and variability of CO_2 and its sources and sinks.

Current estimates of CO_2 flux from inverse methods rely mainly on ground-based data (Baker et al., 2006). Errors in the estimation of regional fluxes from Africa and South America are particularly large because ground-based monitoring stations are sparsely located in those regions. Spectroscopic remote sensing from space is capable of acquiring data that cover the globe and hence is expected to reduce errors in the CO_2 flux estimation using inverse modeling. To improve annual flux estimates on a sub-continental scale, the required precision of monthly averaged column-averaged volume mixing ratio of carbon dioxide (X_{CO2}) is less than 1% on a 8° × 10° grid without biases (Rayner and O'Brien, 2001; Houweling et al., 2004; Miller et al., 2007). For this purpose, satellite-based data products must be validated by higher-precision data obtained independently using ground-based or aircraft measurements (Chahine et al., 2005; Sussmann et al., 2005; Dils et al., 2006; Schneising et al., 2008; Kulawik et al., 2010).

In this study, the Greenhouse gases Observing SATellite (GOSAT) data products retrieved by the National Institute for Environmental Studies (NIES) are compared with ground-based high resolution Fourier Transform Spectrometer (g-b FTS) data calibrated to the World Meteorological Organization (WMO) scale. In Sect. 2, we present an overview of the GOSAT project, GOSAT instruments and observations, and retrievals from the GOSAT Thermal And Near-infrared Sensor for carbon Observation Fourier Transform Spectrometer, measuring in the Short-Wavelength InfraRed (TANSO-FTS SWIR). Reference data measured with g-b FTS are described in Sect. 3. Finally, characteristics of GOSAT SWIR products and preliminary results compared with the reference data are presented in Sect. 4.

AMTD
3, 5613–5643, 2010

2 Overview of GOSAT, the GOSAT instruments, and data products retrieved from GOSAT TANSO-FTS SWIR observations

2.1 GOSAT

The Greenhouse Gases Observing Satellite "IBUKI" (GOSAT), launched on 23 January 2009, is the world's first satellite dedicated to measuring the atmospheric concentrations of CO_2 and CH_4 from space. The GOSAT Project is a joint effort of the Ministry of the Environment (MOE), the National Institute for Environmental Studies (NIES), and the Japan Aerospace Exploration Agency (JAXA). NIES is responsible for (1) developing the retrieval of greenhouse gas concentrations (Level 2 products) from satellite and auxiliary data, (2) validating the retrieved greenhouse gas concentrations, and (3) producing higher-level processing such as monthly averaged X_{CO2} and X_{CH4} (Level 3 products) and Level 4 carbon flux estimates. The primary purpose of the GOSAT is to make more accurate estimates of these fluxes on sub-continental scales (several thousand square kilometers) and contributing toward the broader effort of environmental monitoring of ecosystem carbon balance. Further, through research using the GOSAT product, new knowledge will be accumulated on the global distribution of greenhouse gases and their temporal variations, as well as the global carbon cycle and its influence on climate. These new findings will be utilized to improve predictions of future climate change and its impacts.

2.2 GOSAT instruments and observation methods

Details of the GOSAT instruments have been described by Kuze et al. (2009). GOSAT is placed in a sun-synchronous orbit with an equator crossing time of about 13:00 LT (local time), with an inclination angle of 98 degrees. GOSAT flies at an altitude of approximately 666 km and completes an orbit in about 100 min. The spacecraft returns

AMTD
3, 5613–5643, 2010

to observe the same point on Earth every three days. The instruments onboard the satellite are TANSO-FTS and the TANSO Cloud and Aerosol Imager (TANSO-CAI).

TANSO-FTS has a Michelson interferometer that was custom designed and built by ABB-Bomem, Quebec, Canada. Spectra are obtained in four bands: band 1 spanning 0.758–0.775 µm (12 900–13 200 cm^{-1}) with 0.37 cm^{-1} or better spectral resolution, and bands 2–4, spanning 1.56–1.72, 1.92–2.08, and 5.56–14.3 µm (5800–6400, 4800–5200, and 700–1800 cm^{-1}, respectively) with 0.26 cm^{-1} or better spectral resolution. The TANSO-FTS instantaneous field of view is ~15.8 mrad corresponding to a nadir footprint diameter of about 10.5 km at sea level. The nominal single-scan data acquisition time is 4 s.

TANSO-FTS observes solar light reflected from the earth's surface as well as the thermal radiance emitted from the atmosphere and the surface. The former (SWIR region) is observed in bands 1 to 3 of the FTS in the daytime only, and the latter (Thermal InfraRed, TIR, region) is captured in band 4 during both the day and the night. The surface reflection characteristics of land and water differ significantly. The land is close to Lambertian, whereas the ocean is much more specular. TANSO-FTS observes scattered sunlight over land using a nadir-viewing observation mode, and over ocean using a sunglint observation mode.

TANSO-CAI is a radiometer and observes the state of the atmosphere and the surface during daytime. The image data from CAI are used to determine cloud properties over an extended area that includes the FTS' field of view as described by Ishida and Nakajima (2009). As part of the retrieval, cloud characteristics and aerosol amounts are also retrieved. This information can be used to reject cloudy scenes and correct the influence of aerosols on the retrieved X_{CO2} and X_{CH4}.

Over the three-day orbital repeat period, TANSO-FTS takes several tens of thousands of observations that cover the globe. Since the retrievals are limited to areas under clear sky conditions, only about ten percent of the spectra obtained by TANSO-FTS can be used for the retrieval of CO_2 and CH_4. Nevertheless, the number of remaining data points far surpasses the current number of ground monitoring stations

AMTD
3, 5613–5643, 2010

used for analysis in the World Data Center for Greenhouse Gases (WDCGG), which is below 200 (WMO, 2009). GOSAT serves to fill in the blanks in the ground observation network.

2.3 Products retrieved from GOSAT TANSO-FTS SWIR spectra

The analysis of the TANSO-FTS SWIR spectra is described in detail by Yoshida et al. (2010). Briefly, absorption spectra are used together to retrieve CO_2 and CH_4 column abundances. From all spectra observed with TANSO-FTS SWIR, only those measured without cloud interference are selected for further processing. Based on the absorption characteristics of each gas, the selected spectra are used to retrieve column abundances of CO_2 and CH_4 (Level 2 product). Variations in the CO_2 concentration are most obvious near the surface of the earth. The CO_2 absorption bands near 1.6 µm and 2.0 µm provide information on the near-surface concentrations. The absorption band around 14 µm is used to obtain information on the profiles of CO_2 and CH_4, mainly at altitudes above 2 km (Saitoh et al., 2009).

Validation of the TANSO-FTS SWIR Level 2 data product is critical since the data are used for generating Level 3 and Level 4 products. GOSAT Level 2 products are evaluated against high-precision data obtained independently using ground-based or aircraft observations. Here we compare the GOSAT SWIR X_{CO2} and X_{CH4} results with those data obtained with ground-based high-resolution FTSs (g-b FTSs).

3 Reference data measured with g-b FTSs for GOSAT product validation

3.1 X_{CO2} and X_{CH4} retrieval from spectra measured with g-b FTSs

Spectra measured with g-b FTS are analyzed using the GFIT nonlinear least squares spectral fitting algorithm developed at the Jet Propulsion Laboratory (Toon et al., 1992; Wunch et al., 2010b), which is used for retrievals across all stations that comprise the

AMTD
3, 5613–5643, 2010

Total Carbon Column Observing Network (TCCON; Wunch et al., 2010b). Here, we use the GFIT 7 March 2009 release.

The column-averaged volume mixing ratio of CO_2 (X_{CO2}) is defined to be the ratio of the CO_2 column amount to the dry air column amount. To calculate the dry air column, we use the measured O_2 column, divided by the known dry air mole fraction of O_2 (0.2095). The O_2 column is measured simultaneously with the CO_2 column using the spectral band covering 1.25–1.29 µm. X_{CO2} is obtained from:

$$X_{CO2} = 0.2095 \left(CO_2 \text{ column}/O_2 \text{ column}\right)$$

Ratioing by O_2 minimizes systematic and correlated errors present in both retrieved columns like pointing error, surface pressure uncertainty, instrument line shape uncertainty, H_2O vapor uncertainty, zero level offsets and solar intensity variation (e.g. thin clouds).

The precision of g-b FTS measurement of X_{CO2} is better than 0.2% under clear sky conditions (Washenfelder et al., 2006; Ohyama et al., 2009; Wunch et al., 2010b; Messerschmidt et al., 2010). All TCCON X_{CO2} data are corrected for an airmass-dependent artifact (Wunch et al., 2010b). Aircraft profiles obtained over many of these sites are used to determine an empirical scaling to place the TCCON data on the WMO standard reference scale. The scaling factors of X_{CO2} and X_{CH4} are 1.011 and 1.022, respectively. The uncertainty of X_{CO2} and X_{CH4} associated with the g-b FTS measurement is estimated to be 0.8 ppm (~0.2%) and 4 ppb (~0.2%) by comparing the TCCON retrievals with many different aircraft profiles (Wunch et al., 2010a).

3.2 FTS sites used for validation

The g-b FTS data at 9 sites are used in this analysis. Figure 1 shows the location of the FTS sites which are used in the present study. FTS sites are located in Asia, Oceania, Europe, and North America. Table 1 summarizes the spatial coordinates of those stations.

AMTD
3, 5613–5643, 2010

4 Results of initial validation

4.1 GOSAT product selection for validation

The GOSAT SWIR X_{CO2} and X_{CH4} products used here are Ver.01.xx. The retrieval algorithm for Ver.01.xx uses band 1 (12 900–13 200 cm^{-1}) and band 2 (5800–6400 cm^{-1}) to simultaneously estimate X_{CO2} and X_{CH4}. In addition, the water vapor profile and aerosol optical depth (AOD) at a wavelength of 1.6 µm are retrieved. Band 3 is used for selecting scenes with cirrus clouds which CAI can not detect (Yoshida et al., 2010). The X_{CO2} and X_{CH4} data shown here (general public users, or GU subset) are filtered for AOD less than 0.5. As a plane-parallel atmosphere is assumed in the retrieval, data with solar zenith angles greater than 70° are not processed, and data over high mountain ranges such as the Rockies, the Andes, and the Himalayan mountains are removed.

4.2 Global distribution of X_{CO2} and X_{CH4}

Figures 2 and 3 show the global distribution of GOSAT SWIR X_{CO2} and X_{CH4} measured in April and October 2009. When several GOSAT data were retrieved at the same observation point in the month, the latest retrieved value was overwritten in Figs. 2 and 3. There are retrievals that satisfy the filter criteria over North Africa, the Arabian Peninsula, and Australia. Data over land are obtained mainly for 10–60° N and 15–45° S in April, and 10–50° N and 0–50° S in October. Data over ocean are retrieved in the regions of 10° S–30° N in April and 40° S–10° N in October by observing the specular reflection of sunlight in the direction of sunglint.

X_{CO2} in April is generally higher in the Northern Hemisphere than the Southern Hemisphere (Fig. 2). This is because plant photosynthesis in the Northern Hemisphere is not yet competitive with respiration in April. In October, similar X_{CO2} is observed in both hemispheres. The standard deviations of monthly mean X_{CO2} is about 1% for a 10° × 10° grid over Australia, where gradients are anticipated to be very small.

AMTD
3, 5613–5643, 2010

X_{CH4} in the Northern Hemisphere is higher than in the Southern Hemisphere in both April and October 2009 (Fig. 3). Elevated X_{CH4} is observed from India to Japan in October 2009. These features are similar to those obtained by SCIAMACHY (Frankenberg et al., 2006) and simulated by an inversion model (Bergamaschi et al., 2007).

4.3 Comparisons between g-b FTS data and GOSAT TANSO-FTS SWIR data

GOSAT TANSO-FTS SWIR data are compared with the g-b FTS data at 9 TCCON sites (Fig. 1). We illustrate here the time series of the TANSO-FTS SWIR Level 2 data and g-b FTS data and their scatter diagrams for X_{CO2} and X_{CH4}. The g-b FTS data are the mean values and standard deviations (one sigma) measured at each FTS site within 30 min of GOSAT overpass time (at most sites, around 13:00 LT). The GOSAT data are selected within about one to three degrees rectangular area centered at each FTS site depending on the geophysical distribution of land and sea. As much as possible, we used only the GOSAT data retrieved over flat land.

4.3.1 X_{CO2}

The time series of the GOSAT and g-b FTS data for X_{CO2} are shown on the left and their scatter diagram on the right in Figs. 4 and 5g,h. In the scatter diagram, we plotted data when g-b FTS data were collected within 30 min of the GOSAT overpass time and corresponding GOSAT X_{CO2} values were successfully retrieved. Only a few GOSAT data are available for comparison with Bialystok, Garmisch, Park Falls and Lauder. Darwin FTS data were not obtained since 2010 due to mechanical problems with the sun tracker. X_{CO2} retrieved from GOSAT SWIR measured near Orleans, Lamont and Tsukuba sites are higher in boreal spring and lower in autumn (Figs. 4b, 5e and f). Although GOSAT data are generally biased low compared with the g-b FTS, similar seasonal variations are observed. A clear seasonality over the Northern Hemisphere can also be seen in the horizontal maps of Fig. 2. In contrast, the seasonal variation

AMTD
3, 5613–5643, 2010

of g-b FTS X_{CO2} in the Southern Hemisphere (i.e., Darwin, Wollongong, and Lauder) is weak (Fig. 5g,h and i) as expected due to smaller contribution of the continents.

Figure 6 shows the scatter diagram between the GOSAT data and the g-b FTS data for all sites, and Table 2 summarizes the difference of the GOSAT data to the g-b FTS data at each site. The difference of the GOSAT data to the g-b FTS data is -8.85 ± 4.75 ppm or -2.3 ± 1.2%.

4.3.2 X_{CH4}

The time series of the GOSAT and g-b FTS data for X_{CH4} are shown on the left and their scatter diagrams on the right in Figs. 7 and 8. The GOSAT retrievals are quite similar to the g-b FTS data for each site. Furthermore, the bias of X_{CH4} is smaller than that of X_{CO2}. In Lamont and Orleans, X_{CH4} levels obtained from GOSAT SWIR are higher in boreal autumn. The g-b FTS data of X_{CH4} over Tsukuba have a peak in summer rather than autumn.

Figure 9 shows the scatter diagram between the GOSAT data and the g-b FTS data for all sites. The difference between the GOSAT data and the g-b FTS data at each site is shown in Table 3. The difference of the GOSAT data to the g-b FTS data is -20.4 ± 18.9 ppb or -1.2 ± 1.1%.

4.4 Latitudinal distributions of zonal averaged GOSAT SWIR X_{CO2} and X_{CH4}

In Sect. 4.3, g-b FTS data recorded within 30 min of the GOSAT overpass were used for the validation. To obtain larger number of samples and depict the latitudinal features, we calculated monthly mean X_{CO2} and X_{CH4} of g-b FTS data obtained within 30 min of the time when GOSAT is supposed to overpass for all days, including the days when GOSAT does not overpass each site. In addition, monthly mean values of zonal averaged GOSAT data, based on all data obtained, are calculated in each 15 degree latitudinal band.

AMTD
3, 5613–5643, 2010

Latitudinal distributions of monthly means of zonal averaged GOSAT SWIR and g-b FTS data of X_{CO2} in April and October 2009 are shown in Fig. 10. Both data sets show that X_{CO2} is higher in the Northern Hemisphere compared with the Southern Hemisphere in April and the difference between the hemispheres is small in October. The difference of X_{CO2} between April and October is about 5 ppm in the northern mid latitudes for both data sets. The zonal means of GOSAT data are reasonably consistent with those of the reference values.

Figure 11 shows latitudinal distributions of monthly means of zonal averaged GOSAT SWIR and g-b FTS data of X_{CH4} for April and October 2009. X_{CH4} is characterized by relatively high concentration in the Northern Hemisphere in April and October. Moreover, the bias is smaller than that of X_{CO2}. In particular, concentration of X_{CH4} of GOSAT data is a good agreement with that of g-b FTS sites in April. Both X_{CH4} data in October are similar distribution, though a striking difference is seen near 50–60° N.

5 Discussion

In this study, we performed the validation of GOSAT TANSO-FTS SWIR X_{CO2} and X_{CH4}. In Ver.01.xx, the influence of aerosols has been markedly reduced compared with earlier versions of the retrievals (Yokota et al., 2009). However, bias due to aerosols and thin cirrus clouds still exists because the anomalously low X_{CO2} retrievals as illustrated in Fig. 2. In the future, we plan to investigate interferences by aerosols and thin cirrus clouds using aerosol lidars and/or sky-radiometers at selected FTS sites.

The negative bias of about 9 ppm or 2.3% in the GOSAT TANSO-FTS SWIR data of X_{CO2} is not still understood. It may result from unknown spectroscopic parameters of O_2 and CO_2 or error in the TANSO-FTS calibration. In the case of the GOSAT SWIR data of X_{CH4}, the negative bias decreased in the Ver.01.xx compared with the earlier Ver.00.yy when the spectroscopic parameters were changed from Lyulin et al. (2009) to HITRAN 2008 database (Rothman et al., 2009).

AMTD
3, 5613–5643, 2010

The precision of the GOSAT SWIR X_{CO2} and X_{CH4} is considered to be about 1%. The retrieval errors of X_{CO2} and X_{CH4} are on average 2 ppm and 8 ppb or about 0.5% respectively. The retrieval errors include TANSO-FTS SWIR measurement noise, smoothing error and interference error, and the main error is the measurement noise (Yoshida et al., 2010). This means that the other errors of about 0.5% are due to influences of factors such as aerosols and thin cirrus clouds.

6 Conclusions

The GOSAT TANSO-FTS SWIR data of X_{CO2} and X_{CH4} in the Version 01.xx were compared against reference data obtained with the TCCON g-b FTS sites. The GOSAT TANSO-FTS SWIR X_{CO2} and X_{CH4} were biased low by 8.85 ± 4.75 ppm (2.3 ± 1.2%) and 20.4 ± 18.9 ppb (1.2 ± 1.1%) respectively than the reference values. The precision of the GOSAT SWIR X_{CO2} and X_{CH4} retrievals is considered to be about 1%.

Although X_{CO2} is underestimated by approximately 9 ppm, the GOSAT retrievals and g-b FTS data show similar seasonal behaviors over the Northern Hemisphere, higher in spring and lower in autumn. The latitudinal distribution of zonal averaged GOSAT SWIR X_{CO2} and X_{CH4} is broadly consistent with that of the g-b FTS. We plan further study to address the negative bias of the GOSAT SWIR X_{CO2} and X_{CH4} as well as to better understand the influence of aerosols and thin cirrus clouds.

Acknowledgements. We express our sincere thanks to the members of the NIES GOSAT project office, data algorithm team, atmospheric transport modeling team for their useful comments. We thank Nobuyuki Kikuchi in NIES and Komei Yamaguchi in the Japan Weather Association for plotting the data. This work was funded by the Ministry of the Environment in Japan. We also thank NASA's Terrestrial Ecology Program and the Orbiting Carbon Observatory for their support of TCCON, and acknowledge support from the EU within the projects GEOMON and IMECC. The Lauder TCCON measurements are funded by New Zealand Foundation for Research, Science and Technology contracts CO1X0204 and CO1X0406.

AMTD
3, 5613–5643, 2010

References

Baker, D. F., Law, R. M., Gurney, K. R., Rayner, P., Peylin, P., Denning, A. S., Bousquet, P., Bruhwiler, L., Chen, Y.-H., Ciais, P., Fung, I. Y., Heimann, M., John, J., Maki, T., Maksyutov, S., Masarie, K., Prather, M., Pak, B., Taguchi, S., and Zhu, Z.: TransCom 3 inversion intercomparison: Impact of transport model errors on the interannual variability of regional CO_2 fluxes, 1988–2003, Global Biogeochem. Cy., 20, GB1002, doi:10.1029/2004GB002439, 2006.

Bergamaschi, P., Frankenberg, C., Meirink, J. F., Krol, M., Dentener, F., Wagner, T., Platt, U., Kaplan, J. O., Körner, S., Heimann, M., Dlugokencky, E. J., and Goede, A.: Satellite chartography of atmospheric methane from SCIAMACHY on board ENVISAT: 2. Evaluation based on inverse model simulations, J. Geophys. Res., 112, D02304, doi:10.1029/2006JD007268, 2007.

Chahine, M., Barnet, C., Olsen, E. T., Chen, L., and Maddy, E.: On the determination of atmospheric minor gases by the method of vanishing partial derivatives with application to CO_2, Geophy. Res. Lett., 32, L22803, doi:10.1029/2005GL024165, 2005.

Cox, P. M., Betts, R. A., Jones, C. D., Spall, S. A., and Totterdell, I. J.: Acceleration of global warming due to carbon-cycle feedbacks in a coupled climate model, Nature, 408, 184–187, 2000.

Deutscher, N. M., Griffith, D. W. T., Bryant, G. W., Wennberg, P. O., Toon, G. C., Washenfelder, R. A., Keppel-Aleks, G., Wunch, D., Yavin, Y., Allen, N. T., Blavier, J.-F., Jiménez, R., Daube, B. C., Bright, A. V., Matross, D. M., Wofsy, S. C., and Park, S.: Total column CO_2 measurements at Darwin, Australia - site description and calibration against in situ aircraft profiles, Atmos. Meas. Tech., 3, 947–958, doi:10.5194/amt-3-947-2010, 2010.

Dils, B., De Mazière, M., Müller, J. F., Blumenstock, T., Buchwitz, M., de Beek, R., Demoulin, P., Duchatelet, P., Fast, H., Frankenberg, C., Gloudemans, A., Griffith, D., Jones, N., Kerzenmacher, T., Kramer, I., Mahieu, E., Mellqvist, J., Mittermeier, R. L., Notholt, J., Rinsland, C. P., Schrijver, H., Smale, D., Strandberg, A., Straume, A. G., Stremme, W., Strong, K., Sussmann, R., Taylor, J., van den Broek, M., Velazco, V., Wagner, T., Warneke, T., Wiacek, A., and Wood, S.: Comparisons between SCIAMACHY and ground-based FTIR data for total columns of CO, CH_4, CO_2 and N_2O, Atmos. Chem. Phys., 6, 1953–1976, doi:10.5194/acp-6-1953-2006, 2006.

AMTD
3, 5613–5643, 2010

Frankenberg, C., Meirink, J. F., Bergamaschi, P., Goede, A. P. H., Heimann, M., Körner, S., Platt, U., van Weele, M., and Wagner, T.: Satellite chartography of atmospheric methane from SCIAMACHY on board ENVISAT: Analysis of the years 2003 and 2004, J. Geophys. Res., 111, D07303, doi:10.1029/2005JD006235, 2006.

Houweling, S., Breon, F.-M., Aben, I., Rödenbeck, C., Gloor, M., Heimann, M., and Ciais, P.: Inverse modeling of CO_2 sources and sinks using satellite data: a synthetic inter-comparison of measurement techniques and their performance as a function of space and time, Atmos. Chem. Phys., 4, 523–538, doi:10.5194/acp-4-523-2004, 2004.

Intergovernmental Panel on Climate Change (IPCC): Climate change 2007: The Physical Science Basis: Contribution of Working Group I to the Fourth Assessment Report of the Intergovernmental Panel on Climate Change, edited by: Solomon, S., Qin, S., Manning, M., Chen, Z., Marquis, M., Averyt, K. B., Tignor, M., and Miller, H. L., Cambridge University Press, Cambridge, UK and New York, NY, USA, 996 pp., 2007.

Ishida, H. and Nakajima, T. Y.: Development of an unbiased cloud detection algorithm for a spaceborne multispectral imager, J. Geophys. Res., 114, D07206, doi:10.1029/2008JD010710, 2009.

Kulawik, S. S., Jones, D. B. A., Nassar, R., Irion, F. W., Worden, J. R., Bowman, K. W., Machida, T., Matsueda, H., Sawa, Y., Biraud, S. C., Fischer, M. L., and Jacobson, A. R.: Characterization of Tropospheric Emission Spectrometer (TES) CO_2 for carbon cycle science, Atmos. Chem. Phys., 10, 5601–5623, doi:10.5194/acp-10-5601-2010, 2010.

Kuze, A., Suto, H., Nakajima, M., and Hamazaki, T.: Thermal and near infrared sensor for carbon observation Fourier-transform spectrometer on the Greenhouse Gases Observing Satellite for greenhouse gases monitoring, Appl. Optics, 48, 6716–6733, 2009.

Lyulin, O. M., Nikitin, A. V., Perevalov, V. I., Morino, I., Yokota, T., Kumazawa, R., and Watanabe, T.: Measurements of N_2- and O_2-broadening and shifting parameters of methane spectral lines in the 5550–6236 cm^{-1} region, J. Quant. Spectrosc. Ra., 110, 654–668, 2009.

Messerschmidt, J., Macatangay, R., Notholt, J., Petri, C., Warneke, T., and Weinzierl, C.: Side by side measurements of CO_2 by ground-based Fourier transform spectrometry (FTS), Tellus B, 62, 749–758, 2010.

Miller, C. E., Crisp, D., DeCola, P. L., Olsen, S. C., Randerson, J. T., Michalak, A. M., Alkhaled, A., Rayner, P., Jacob, D. J., Suntharalingam, P., Jones, D. B. A., Denning, A. S., Nicholls, M. E., Doney, S. C., Pawson, S., Boesch, H., Connor, B. J., Fung, I. Y., O'Brien, D., Salawitch, R. J., Sander, S. P., Sen, B., Tans, P., Toon, G. C., Wennberg, P. O., Wofsy, S. C., Yung, Y. L.,

AMTD
3, 5613–5643, 2010

and Law, R. M.: Precision requirements for space-based X_{CO2} data, J. Geophys. Res., 112, D10314, doi:10.1029/2006JD007659, 2007.

Ohyama, H., Morino, I., Nagahama, T., Machida, T., Suto, H., Oguma, H., Sawa, Y., Matsueda, H., Sugimoto, N., Nakane, H., and Nakagawa, K.: Column-averaged volume mixing ratio of CO_2 measured with ground-based Fourier transform spectrometer at Tsukuba, J. Geophys. Res., 114, D18303, doi:10.1029/2008JD011465, 2009.

Rayner, P. J. and O'Brien, D. M.: The utility of remotely sensed CO_2 concentration data in surface source inversions, Geophys. Res. Lett., 28, 175–178, 2001.

Rothman, L. S., Gordon, I. E., Barbe, A., Benner, D. C., Bernath, P. F., Birk, M., Boudon, V., Brown, L. R., Campargue, A., Champion, J.-P., Chance, K., Coudert, L. H., Dana, V., Devi, V. M., Fally, S., Flaud, J.-M., Gamache, R. R., Goldman, A., Jacquemart, D., Kleiner, I., Lacome, N., Lafferty, W. J., Mandin, J.-Y., Massie, S. T., Mikhailenko, S. N., Miller, C. E., Moazzen-Ahmadi, N., Naumenko, O. V., Nikitin, A. V., Orphal, J., Perevalov, V. I., Perrin, A., Predoi-Cross, A., Rinsland, C. P., Rotger, M., Šimečková, M., Smith, M. A. H., Sung, K., Tashkun, S. A., Tennyson, J., Toth, R. A., Vandaele, A. C., and Auwera, J. V.: The HITRAN 2008 molecular spectroscopic database, J. Quant. Spectrosc. Ra., 110, 533–572, 2009.

Saitoh, N., Imasu, R., Ota, Y., and Niwa, Y.: CO_2 retrieval algorithm for the thermal infrared spectra of the Greenhouse Gases Observing Satellite: Potential of retrieving CO_2 vertical profile from high-resolution FTS sensor, J. Geophys. Res., 114, D17305, doi:10.1029/2008JD011500, 2009.

Schneising, O., Buchwitz, M., Burrows, J. P., Bovensmann, H., Reuter, M., Notholt, J., Macatangay, R., and Warneke, T.: Three years of greenhouse gas column-averaged dry air mole fractions retrieved from satellite - Part 1: Carbon dioxide, Atmos. Chem. Phys., 8, 3827–3853, doi:10.5194/acp-8-3827-2008, 2008.

Sussmann, R., Stremme, W., Buchwitz, M., and de Beek, R.: Validation of ENVISAT/SCIAMACHY columnar methane by solar FTIR spectrometry at the Ground-Truthing Station Zugspitze, Atmos. Chem. Phys., 5, 2419–2429, doi:10.5194/acp-5-2419-2005, 2005.

Sussmann, R., Rettinger, M., and Borsdorff, T.: The new TCCON-FTS site at Garmisch, Germany (47° N, 11° E, 744 m a.s.l.): Set up, first year of operation, and contribution to OCO and GOSAT validation, Geophys. Res. Abstr., 11, EGU2009-8780-2, 2009.

AMTD
3, 5613–5643, 2010

Toon, G. C., Farmer, C. B., Schaper, P. W., Lowes, L. L., and Norton, R. H.: Composition measurements of the 1989 Arctic winter stratosphere by airborne infrared solar absorption spectroscopy, J. Geophys. Res., 97, 7939–7961, doi:10.1029/91JD03114, 1992.

Washenfelder, R. A., Toon, G. C., Blavier, J.-F., Yang, Z., Allen, N. T., Wennberg, P. O., Vay, S. A., Matross, D. M., and Daube, B. C.: Carbon dioxide column abundances at the Wisconsin Tall Tower site, J. Geophys. Res., 111, D22305, doi:10.1029/2006JD007154, 2006.

WMO: The state of greenhouse gases in the atmosphere using global observations through 2008, WMO Greenhouse Gas Bulletin, No. 5, 2009.

World Data Centre for Greenhouse Gases: WMO Global Watch World Data Centre for Greenhouse Gases, http://gaw.kishou.go.jp/wdcgg/wdcgg.html/, last access: December, 2010.

Wunch, D., Toon, G. C., Wennberg, P. O., Wofsy, S. C., Stephens, B. B., Fischer, M. L., Uchino, O., Abshire, J. B., Bernath, P., Biraud, S. C., Blavier, J.-F. L., Boone, C., Bowman, K. P., Browell, E. V., Campos, T., Connor, B. J., Daube, B. C., Deutscher, N. M., Diao, M., Elkins, J. W., Gerbig, C., Gottlieb, E., Griffith, D. W. T., Hurst, D. F., Jiménez, R., Keppel-Aleks, G., Kort, E. A., Macatangay, R., Machida, T., Matsueda, H., Moore, F., Morino, I., Park, S., Robinson, J., Roehl, C. M., Sawa, Y., Sherlock, V., Sweeney, C., Tanaka, T., and Zondlo, M. A.: Calibration of the Total Carbon Column Observing Network using aircraft profile data, Atmos. Meas. Tech., 3, 1351–1362, doi:10.5194/amt-3-1351-2010, 2010a.

Wunch, D., Toon, G. C., Blavier, J.-F. L., Washenfelder, R. A., Notholt, J., Connor, B. J., Griffith, D. W. T., Sherlock, V., and Wennberg, P. O.: The Total Carbon Column Observing Network (TCCON), Philos. T. Roy. Soc. A, in press, 2010b.

Yokota, T., Yoshida, Y., Eguchi, N., Ota, Y., Tanaka, T., Watanabe, H., and Maksyutov, S.: Global concentrations of CO_2 and CH_4 retrieved from GOSAT: First preliminary results, SOLA, 5, 160–163, 2009.

Yoshida, Y., Ota, Y., Eguchi, N., Kikuchi, N., Nobuta, K., Tran, H., Morino, I., and Yokota, T.: Retrieval algorithm for CO_2 and CH_4 column abundances from short-wavelength infrared spectral observations by the Greenhouse Gases Observing Satellite, Atmos. Meas. Tech. Discuss., 3, 4791–4833, doi:10.5194/amtd-3-4791-2010, 2010.

AMTD
3, 5613–5643, 2010

Table 1. g-b FTS sites used for GOSAT product validation.

Site	Country	Coordinate [Lat., Long.]	Alt. [m a.s.l.]	Reference
Bialystok	Poland	53.23° N, 23.025° E	180	Messerschmidt et al. (2010)
Orleans	France	47.965° N, 2.1125° E	130	Messerschmidt et al. (2010)
Garmisch	Germany	47.476° N, 11.063° E	746.6	Sussmann et al. (2009)
Park Falls	USA	45.945° N, 90.273° W	442	Washenfelder et al. (2006)
Lamont	USA	36.604° N, 97.486° W	320	Wunch et al. (2010a,b)
Tsukuba	Japan	36.0513° N, 140.1215° E	31	Ohyama et al. (2009)
Darwin	Australia	12.42445° S, 130.89154° E	32	Deutscher et al. (2010)
Wollongong	Australia	34.4063° S, 150.879° E	30	
Lauder	New Zealand	45.0384° S, 169.684° E	370	

AMTD
3, 5613–5643, 2010

Table 2. Left side: the average and one standard deviation (1 σ) of the difference between GOSAT X_{CO2} and g-b FTS X_{CO2} for the nine TCCON sites. Right side: the average and one standard deviation (1 σ) of the difference normalized to g-b FTS X_{CO2} (given in percent). Note that the number of data listed here indicates the count of valid cases in which g-b FTS data were collected within 30 min of the GOSAT overpass time and corresponding GOSAT X_{CO2} values were successfully retrieved.

Sites	(GOSAT SWIR X_{CO2})–(g-b FTS X_{CO2})			(GOSAT SWIR X_{CO2})–(g-b FTS X_{CO2}) / (g-b FTS X_{CO2})	
	Number of data	Average (ppm)	1 σ (ppm)	Average (%)	1 σ (%)
Bialystok	1	5.01	–	1.32	–
Orleans	14	−12.85	3.79	−3.33	0.99
Garmisch	3	−7.78	3.78	−2.00	0.96
Park Falls	1	−6.05	–	−1.58	–
Lamont	11	−10.31	4.80	−2.65	1.23
Tsukuba	13	−6.38	2.75	−1.64	0.71
Darwin	6	−6.09	2.61	−1.58	0.68
Wollongong	11	−8.77	4.74	−2.28	1.23
Lauder	2	−7.45	0.15	−1.94	0.04
Total	62	−8.85	4.75	−2.29	1.23

AMTD
3, 5613–5643, 2010

Table 3. As in Table 2 except for X_{CH4}.

Sites	(GOSAT SWIR X_{CH4})–(g-b FTS X_{CH4})			(GOSAT SWIR X_{CH4})–(g-b FTS X_{CH4}) (g-b FTS X_{CH4})	
	Number of data	Average (ppm)	1 σ (ppm)	Average (%)	1 σ (%)
Bialystok	1	0.0227	–	1.29	–
Orleans	14	−0.0367	0.0178	−2.06	1.00
Garmisch	3	−0.0114	0.0160	−0.64	0.90
Park Falls	1	−0.0120	–	−0.66	–
Lamont	11	−0.0230	0.0181	−1.28	1.01
Tsukuba	13	−0.0120	0.0115	−0.67	0.64
Darwin	6	−0.0080	0.0089	−0.46	0.51
Wollongong	11	−0.0235	0.0190	−1.34	1.08
Lauder	2	−0.0067	0.0003	−0.39	0.01
Total	62	−0.0204	0.0189	−1.15	1.06

AMTD
3, 5613–5643, 2010

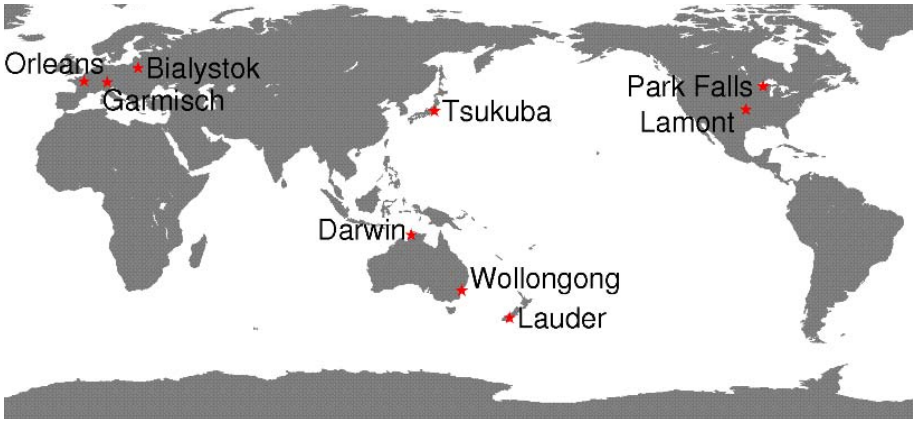

Fig. 1. Ground- based FTS sites used for the GOSAT product validation in the present study.

AMTD
3, 5613–5643, 2010

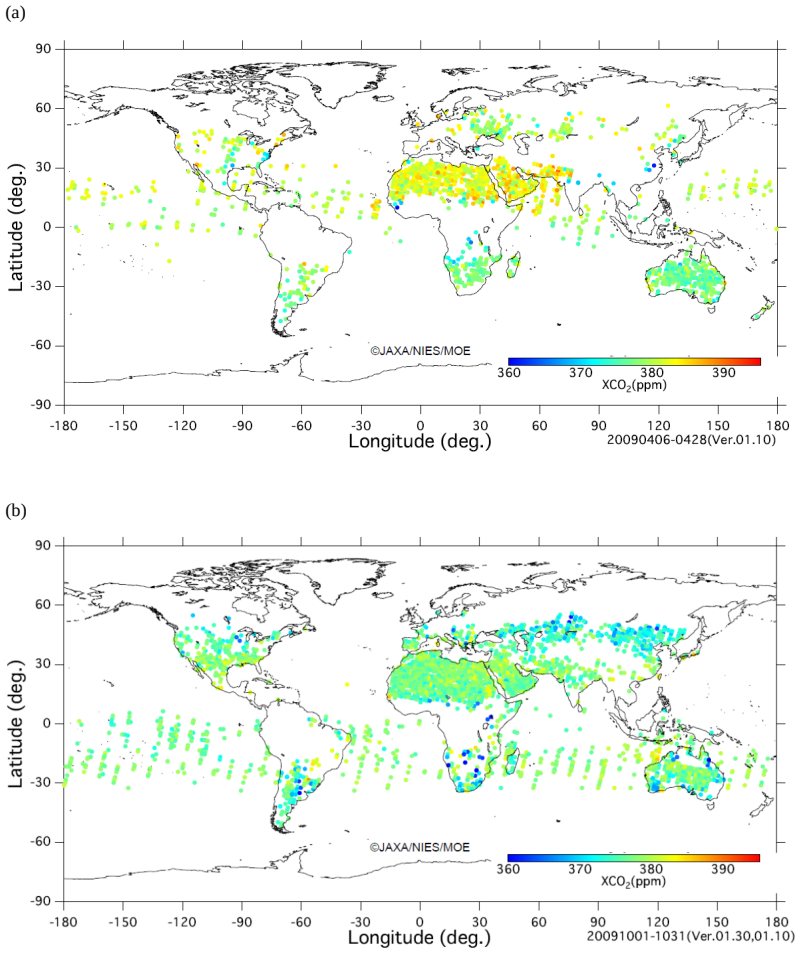

Fig. 2. Global distribution of GOSAT SWIR X_{CO2} for **(a)** April and **(b)** October in 2009.

AMTD
3, 5613–5643, 2010

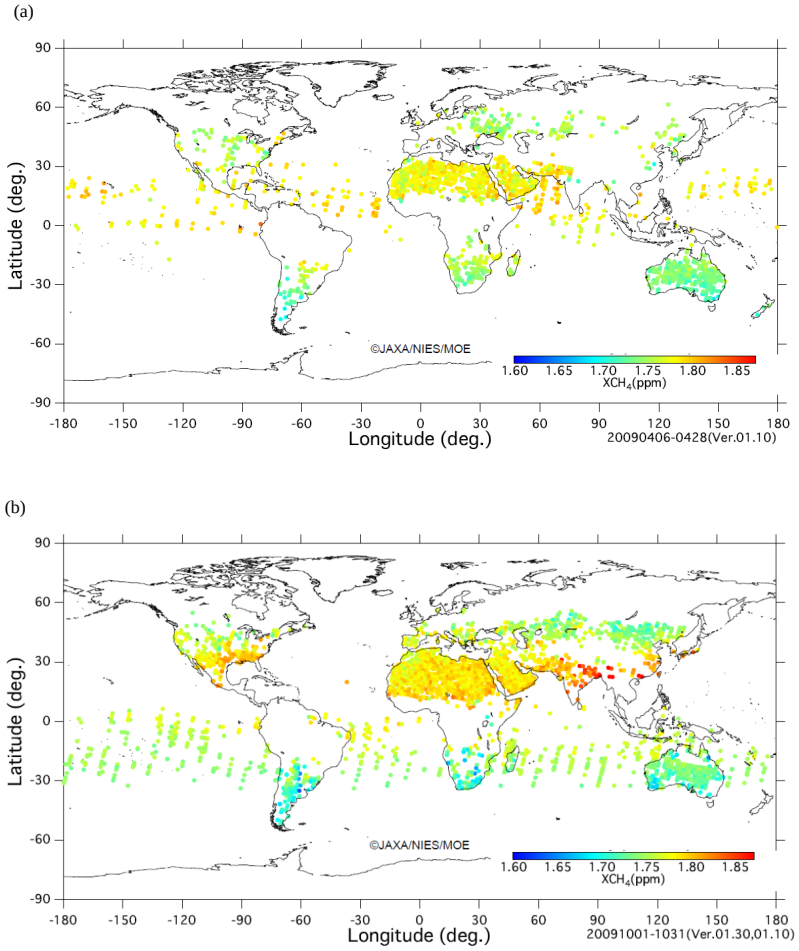

Fig. 3. Global distribution of GOSAT SWIR X_{CH4} for **(a)** April and **(b)** October in 2009.

AMTD
3, 5613–5643, 2010

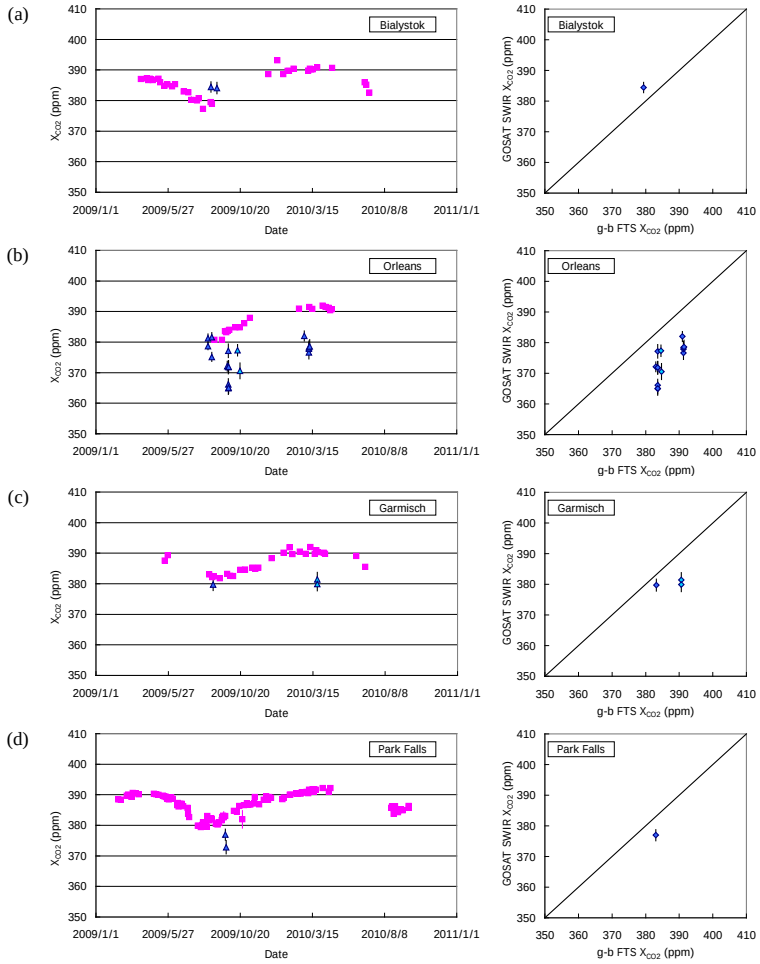

Fig. 4. Time series of GOSAT TANSO-FTS SWIR (blue triangles) and g-b FTS (pink squares) X_{CO2} and their scatter diagram for **(a)** Bialystok, **(b)** Orleans, **(c)** Garmisch, and **(d)** Park Falls.

AMTD
3, 5613–5643, 2010

Preliminary validation of column-averaged volume mixing ratios

I. Morino et al.

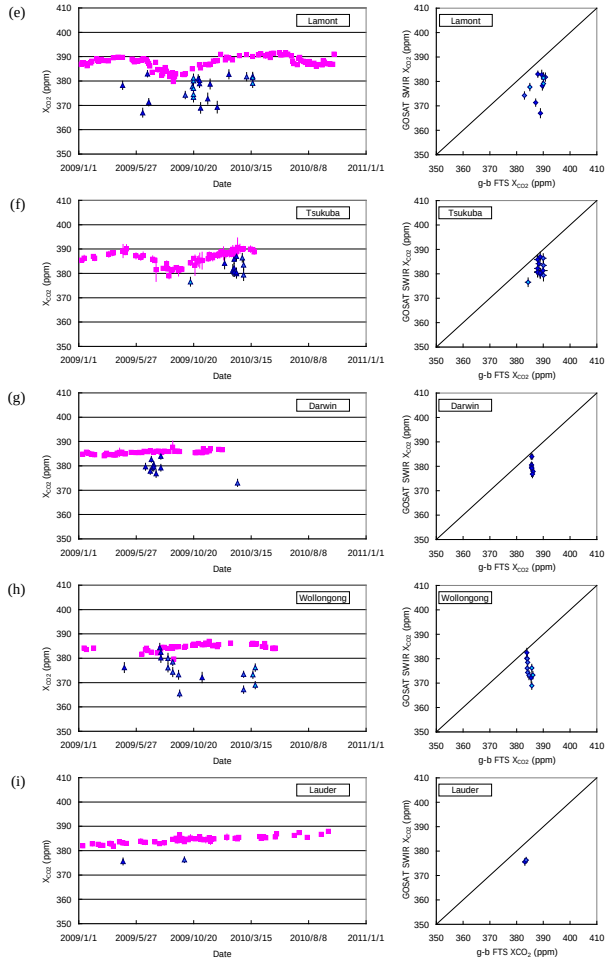

Fig. 5. As in Fig. 4 except for **(e)** Lamont, **(f)** Tsukuba, **(g)** Darwin, **(h)** Wollongong, and **(i)** Lauder.

AMTD
3, 5613–5643, 2010

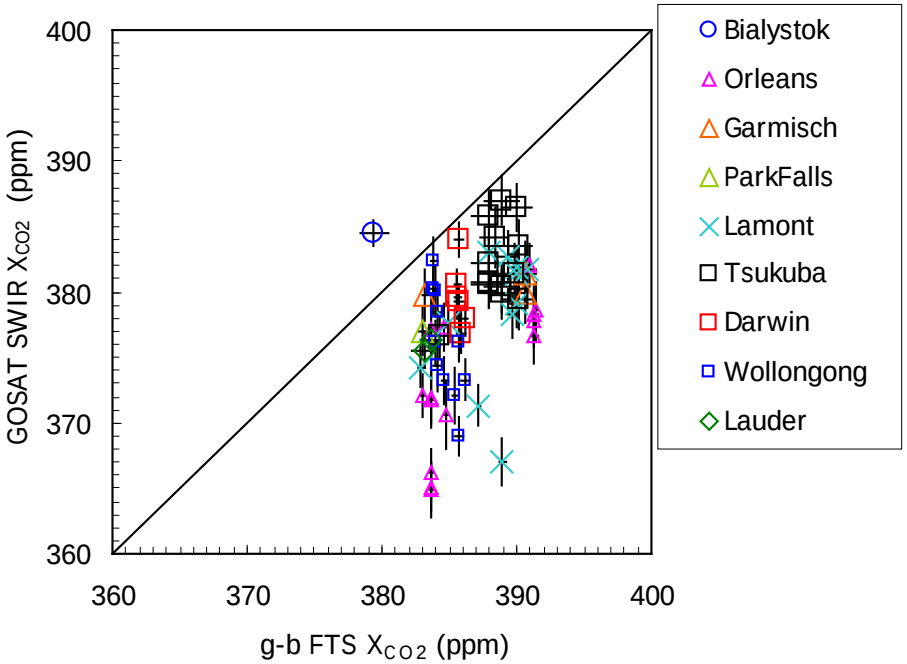

Fig. 6. Scatter diagram between GOSAT TANSO-FTS SWIR and g-b FTS X_{CO2} at FTS sites.

AMTD
3, 5613–5643, 2010

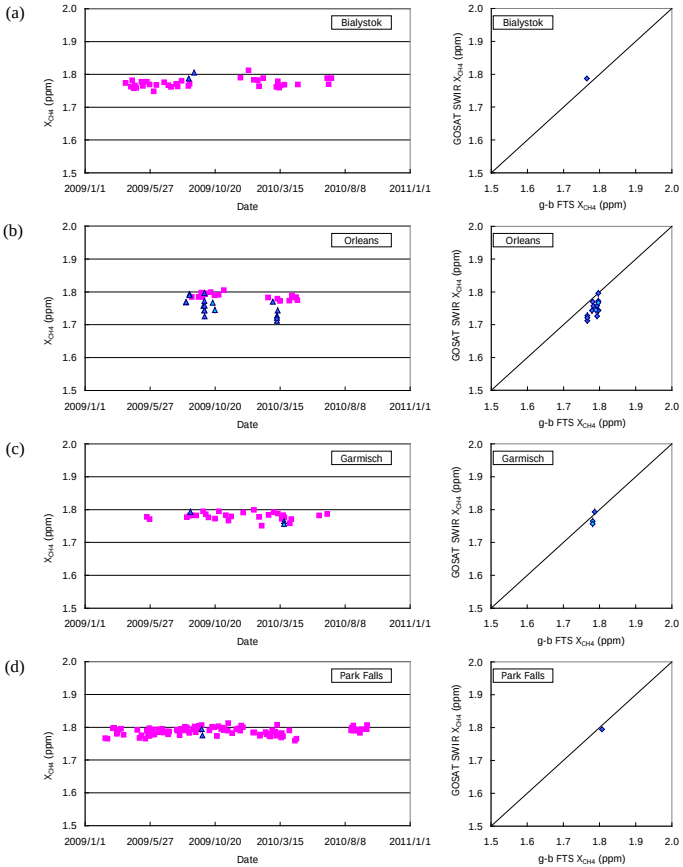

Fig. 7. Time series of GOSAT TANSO-FTS SWIR (blue triangles) and g-b FTS (pink squares) X_{CH4} data and their scatter diagram for **(a)** Bialystok, **(b)** Orleans, **(c)** Garmisch, and **(d)** Park Falls.

AMTD
3, 5613–5643, 2010

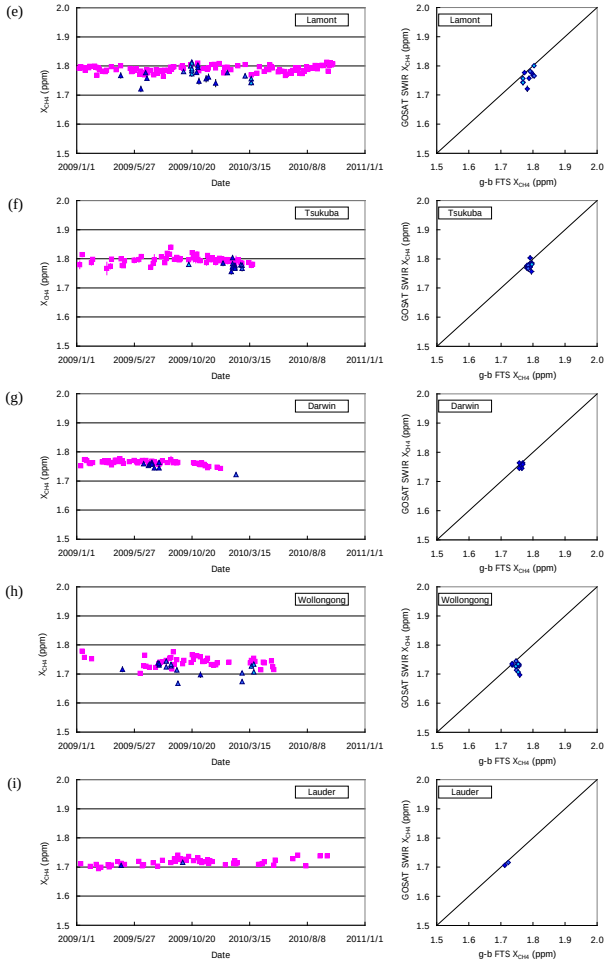

Fig. 8. As in Fig. 7 except for **(e)** Lamont, **(f)** Tsukuba, **(g)** Darwin, **(h)** Wollongong, and **(i)** Lauder.

AMTD
3, 5613–5643, 2010

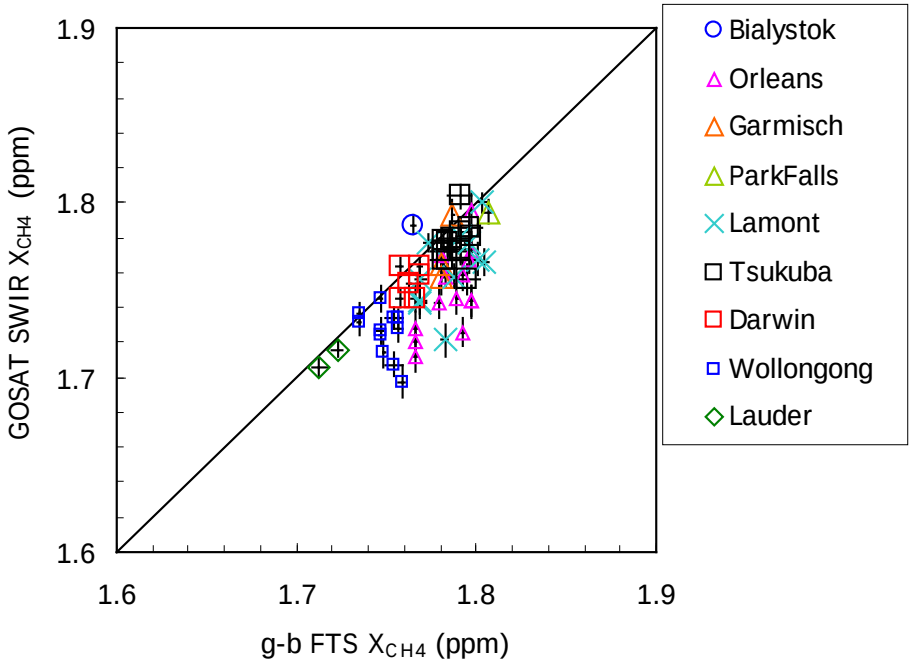

Fig. 9. Scatter diagram between GOSAT TANSO-FTS SWIR and g-b FTS X_{CH4} at FTS sites.

AMTD
3, 5613–5643, 2010

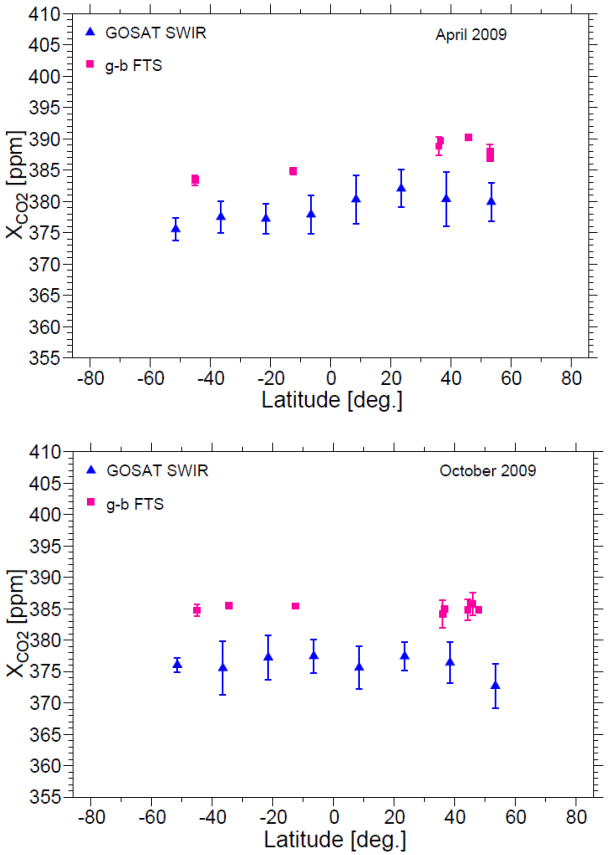

Fig. 10. Latitudinal distributions of monthly means of zonal averaged GOSAT X_{CO2} for each 15 latitudinal band in April and October 2009 (blue triangles). The monthly means of g-b FTS data observed during local time of about 12:30–13:30 h are shown by pink squares. Vertical bars indicate the standard deviation.

AMTD
3, 5613–5643, 2010

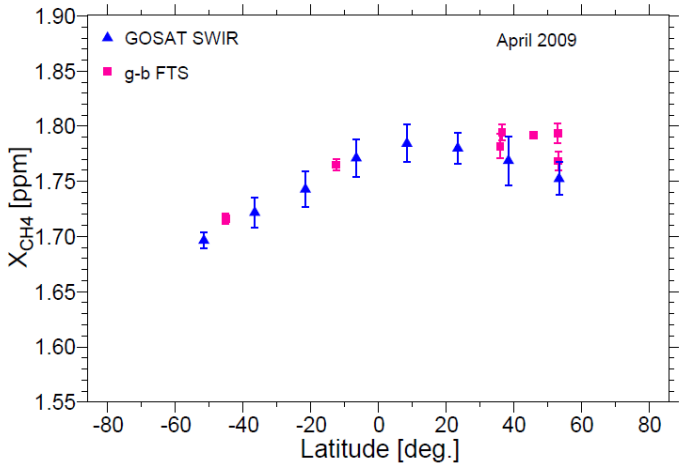

Fig. 11. As Fig. 10 but for X_{CH4}.

AMTD
3, 5613–5643, 2010